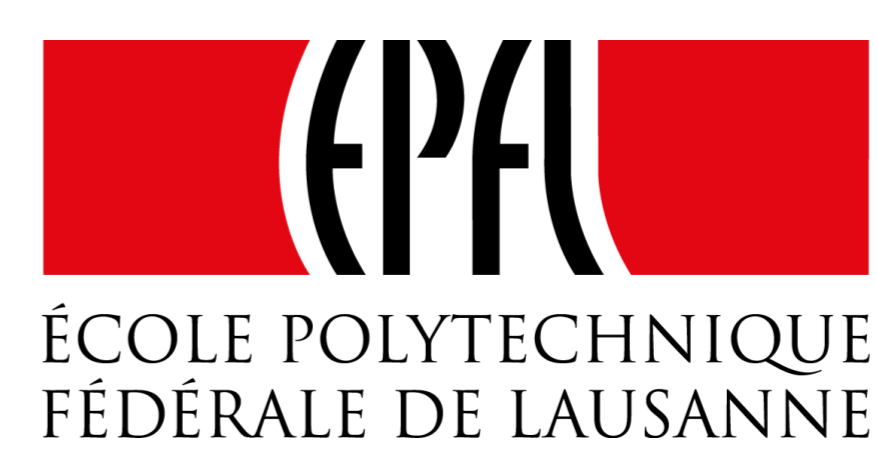


# Effects of plasma shaping on tokamak scrape-off layer turbulence

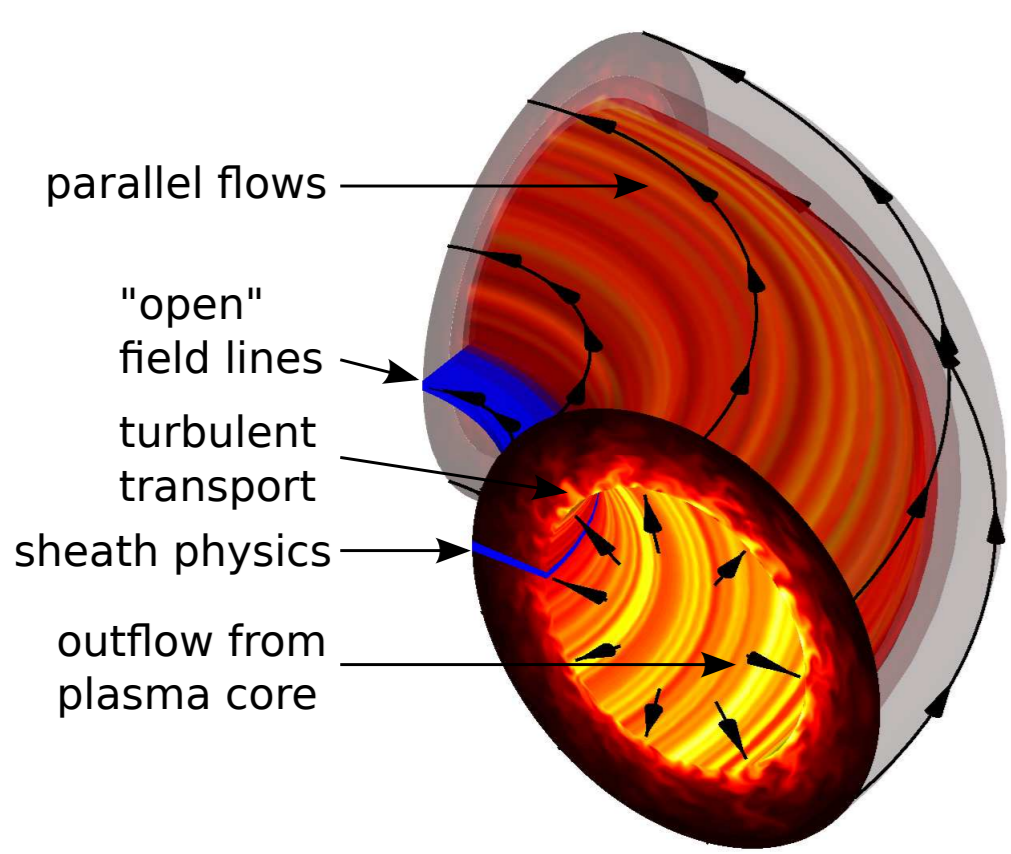
F. Riva, E. Lanti, F. D. Halpern, S. Jolliet, P. Ricci

École Polytechnique Fédérale de Lausanne (EPFL), Swiss Plasma Center, CH-1015 Lausanne, Switzerland



SWISS PLASMA CENTER

## Introduction

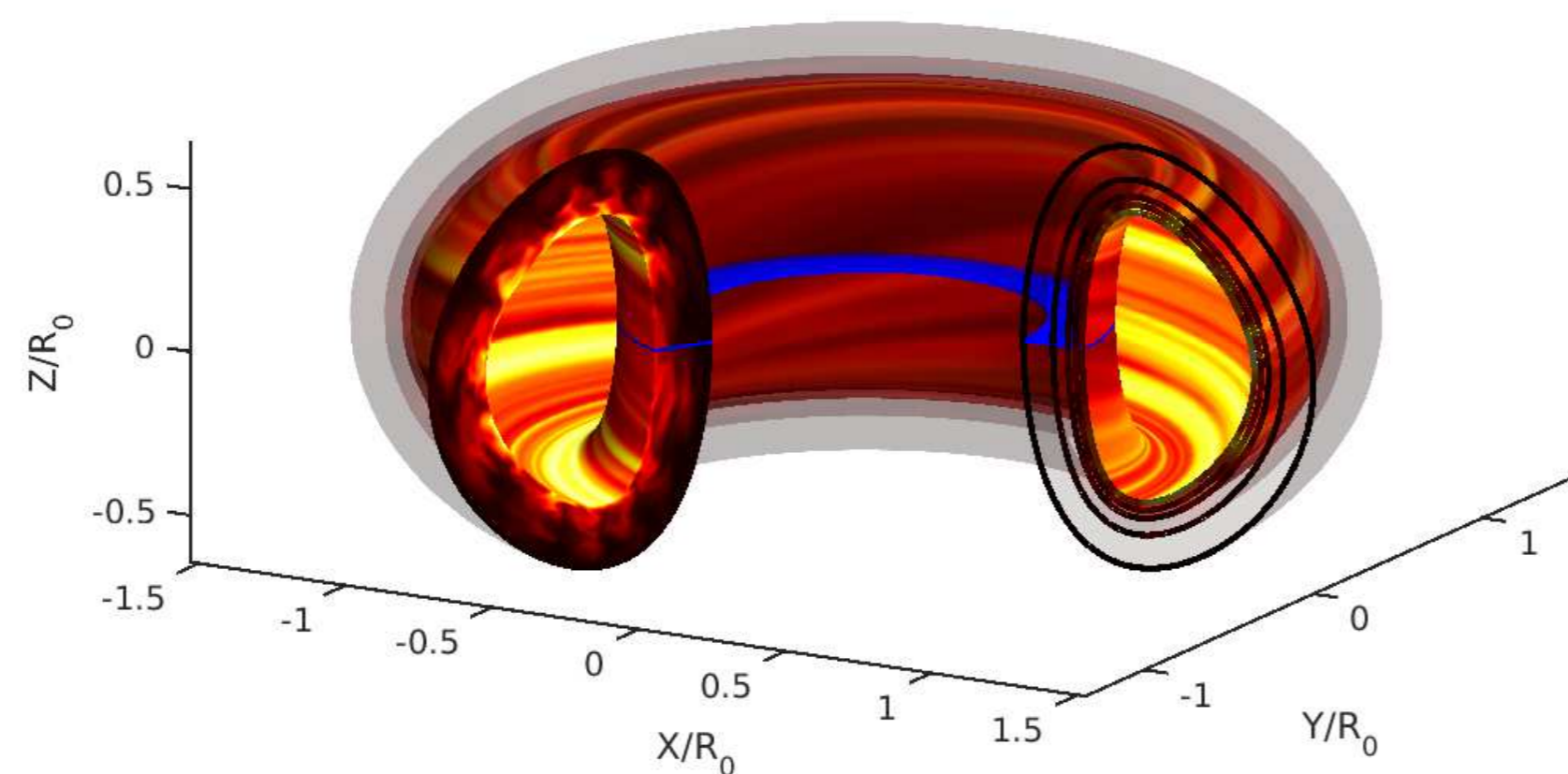


- In Scrape-Off Layer (SOL) of tokamaks, **magnetic field lines intersect the walls** of the fusion device
- Heat and particles** flow along magnetic field lines and are **exhausted to the vessel**

The **Global Braginskii Solver (GBS)** code: a 3D, two-fluid, flux-driven, global turbulence code in limited geometry used to study plasma turbulence in the SOL

## Development and achievements of GBS

- Achievements:
  - Non-linear turbulent regimes in the SOL
  - SOL width scaling as a function of dimensionless / engineering plasma parameters
  - Origin and nature of intrinsic toroidal plasma rotation in the SOL
  - Mechanisms regulating the SOL equilibrium electrostatic potential
- In the past: simulations in **circular limited configuration**
- Described here: **generalization** of the GBS magnetic geometry to include **Shafranov shift**, plasma **elongation**, and non-zero **triangularity**



## The Global Braginskii Solver (GBS) code

- Two-fluid Drift-reduced Braginskii equations**,  $d/dt \ll \omega_{ci}$ :

$$\begin{aligned} \text{Continuity: } \frac{\partial n}{\partial t} &= -\frac{\rho_*^{-1}}{B} [\phi, n] + \frac{2}{B} [C(p_e) - nC(\phi)] - \nabla \cdot (n v_{\parallel e} \mathbf{b}) + S_n \\ \text{Charge conservation: } \frac{\partial \omega}{\partial t} &= -\frac{\rho_*^{-1}}{B} [\phi, \omega] - v_{\parallel i} \nabla_{\parallel} \omega + \frac{B^2}{n} \nabla \cdot (\mathbf{j}_{\parallel} \mathbf{b}) + \frac{2B}{n} C(p_e) \\ \text{Ohm's law: } \frac{\partial v_{\parallel e}}{\partial t} &= -\frac{\rho_*^{-1}}{B} [\phi, v_{\parallel e}] - v_{\parallel e} \nabla_{\parallel} v_{\parallel e} + \frac{m_i}{m_e} \left( \nu \frac{j_{\parallel}}{n} + \nabla_{\parallel} \phi - \frac{1}{n} \nabla_{\parallel} p_e - 0.71 \nabla_{\parallel} T_e \right) \\ \text{Parallel momentum: } \frac{\partial v_{\parallel i}}{\partial t} &= -\rho_*^{-1} [\phi, v_{\parallel i}] - v_{\parallel i} \nabla_{\parallel} v_{\parallel i} - \frac{1}{n} \nabla_{\parallel} p_e \\ \text{Electron temperature: } \frac{\partial T_e}{\partial t} &= -\frac{\rho_*^{-1}}{B} [\phi, T_e] - v_{\parallel e} \nabla_{\parallel} T_e + \frac{4 T_e}{3 B} \left[ \frac{C(p_e)}{n} + \frac{5}{2} C(T_e) - C(\phi) \right] \\ &\quad + \frac{2}{3} T_e \left[ 0.71 \frac{\nabla \cdot (\mathbf{j}_{\parallel} \mathbf{b})}{n} - \nabla \cdot (v_{\parallel e} \mathbf{b}) \right] + S_{T_e} \end{aligned}$$

- Equations implemented in **GBS**, system closed by  $\omega = \nabla_{\perp}^2 \phi$  [Ricci *et al.*, PPCF 2012]
- System completed with a set of **first-principles boundary conditions** applicable at the magnetic pre-sheath entrance where the magnetic field lines intersect the limiter [Loizu *et al.*, PoP 2012]
- Note:  $L_{\perp} \rightarrow \rho_s$ ,  $L_{\parallel} \rightarrow R_0$ ,  $t \rightarrow R_0/c_s$ ,  $\nu \rightarrow ne^2 R_0 / (m_i \sigma_{\parallel} c_s)$  normalization

## GBS operators

- The **magnetic geometry** allows to compute **GBS operators**

$$\begin{aligned} [\phi, A] &= \mathbf{b} \cdot (\nabla \phi \times \nabla A) = \frac{1}{\mathcal{J}} \epsilon^{ijk} b_i \frac{\partial \phi}{\partial \xi^j} \frac{\partial A}{\partial \xi^k} \\ \nabla_{\parallel} A &= \mathbf{b} \cdot \nabla = b^j \frac{\partial A}{\partial \xi^j} \\ \nabla_{\perp}^2 A &= -\nabla \cdot [\mathbf{b} \times (\nabla \times A)] = \frac{1}{\mathcal{J}} \frac{\partial}{\partial \xi^k} \left[ \mathcal{J} (g^{ki} - b^k b^i) \frac{\partial A}{\partial \xi^i} \right] \\ C(A) &= \frac{B}{2} [\nabla \times \left( \frac{\mathbf{b}}{B} \right)] \cdot \nabla A = \frac{B}{2 \mathcal{J}} \frac{\partial c_m}{\partial \xi^i} \frac{\partial A}{\partial \xi^i} \\ \nabla \cdot \mathbf{b} &= \frac{1}{\mathcal{J}} \frac{\partial}{\partial \xi^i} (b^i \mathcal{J}) \end{aligned}$$

- Note: use of curvilinear coordinates and of Einstein summation,  $\mathcal{J}$  is the Jacobian of the metric

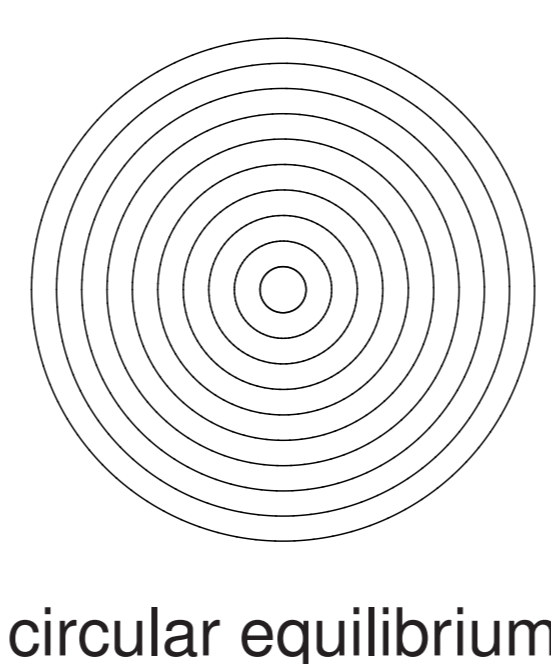
## The magnetic field geometry

- Toroid coordinate system  $(r, \theta, \varphi)$ , general **axisymmetric magnetic field**  $\mathbf{B} = F(\psi) \nabla \varphi + \psi' \nabla r \times \nabla \varphi$
- GBS uses the  $(\theta_*, r, \varphi)$  coordinate system, where  $\theta_*(r, \theta) = \frac{1}{q(r)} \int_0^{\theta} d\theta' \frac{\mathbf{B} \cdot \nabla \varphi}{\mathbf{B} \cdot \nabla \theta'}$  is the straight-field-line angle
- The Grad-Shafranov equation is solved in the  $\epsilon = r/R_0 \rightarrow 0$  limit to obtain  $R(r, \theta)$ ,  $Z(r, \theta)$ , and  $F(\psi)$  as function of  $\kappa$ ,  $\delta$ , and  $q(r)$  [J. P. Graves, PPCF 2013]

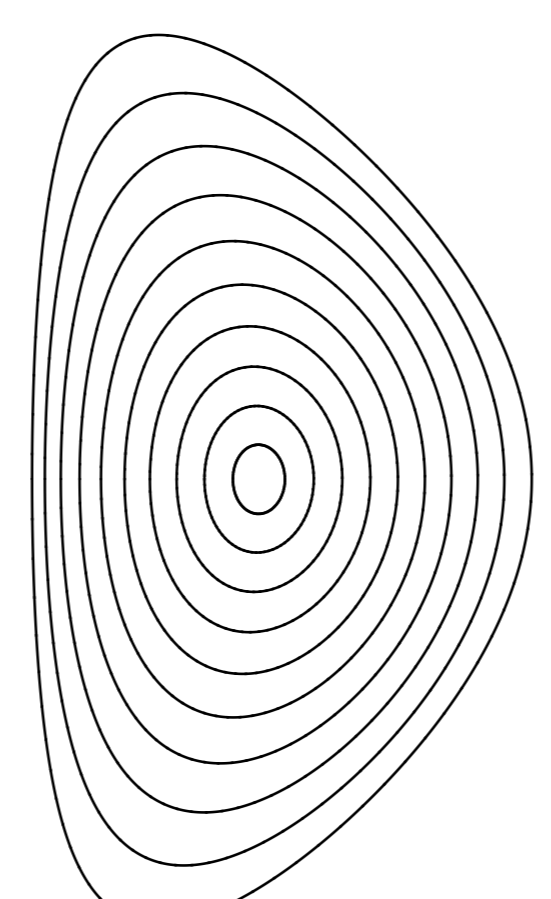
$$R(r, \theta) = R_0 \left( 1 + \epsilon \cos \theta + \frac{\Delta(r)}{R_0} + \sum_{m=2}^3 \frac{S_m(r)}{R_0} \cos[(m-1)\theta] - \frac{P(r)}{R_0} \cos \theta \right)$$

$$Z(r, \theta) = R_0 \left( \epsilon \sin \theta - \sum_{m=2}^3 \frac{S_m(r)}{R_0} \sin[(m-1)\theta] - \frac{P(r)}{R_0} \sin \theta \right)$$

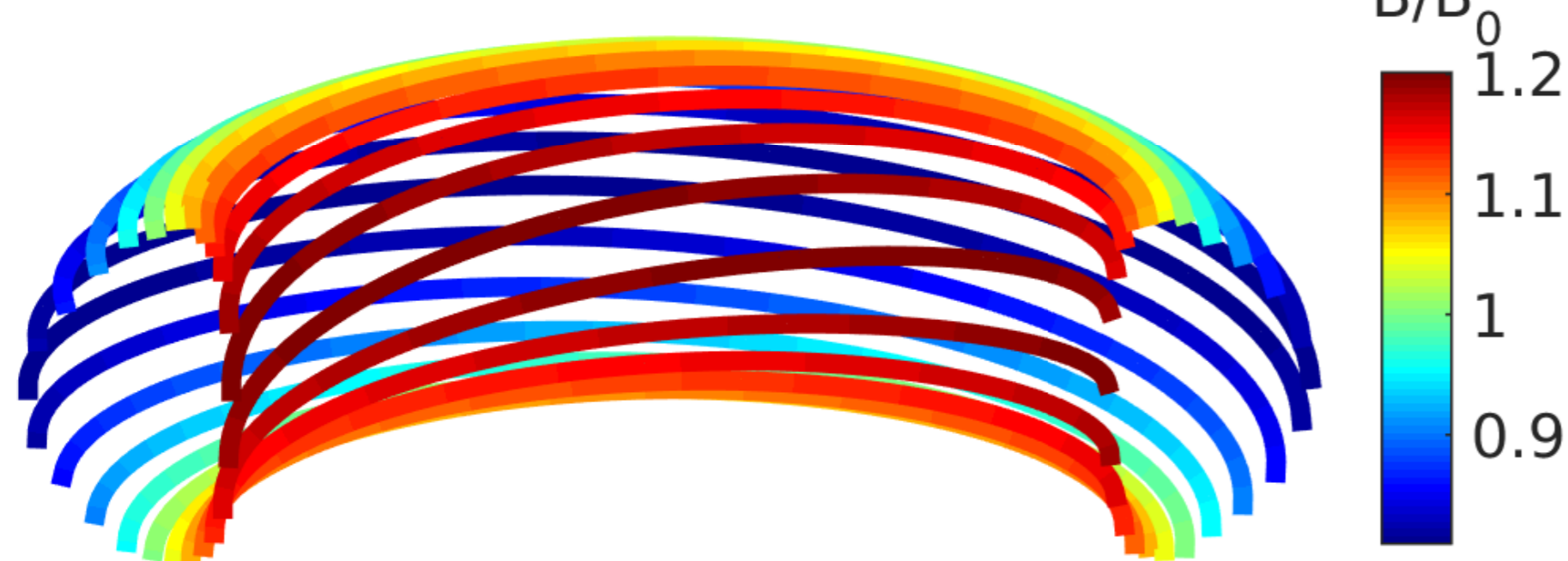
$$F(\psi) = B_0 R_0 \left( 1 - \frac{\epsilon^2}{q(r)^2} \left[ 2 + \frac{q_e - q_0}{q_0} \left( \frac{r}{a} \right)^2 \right] \right)$$



circular equilibrium

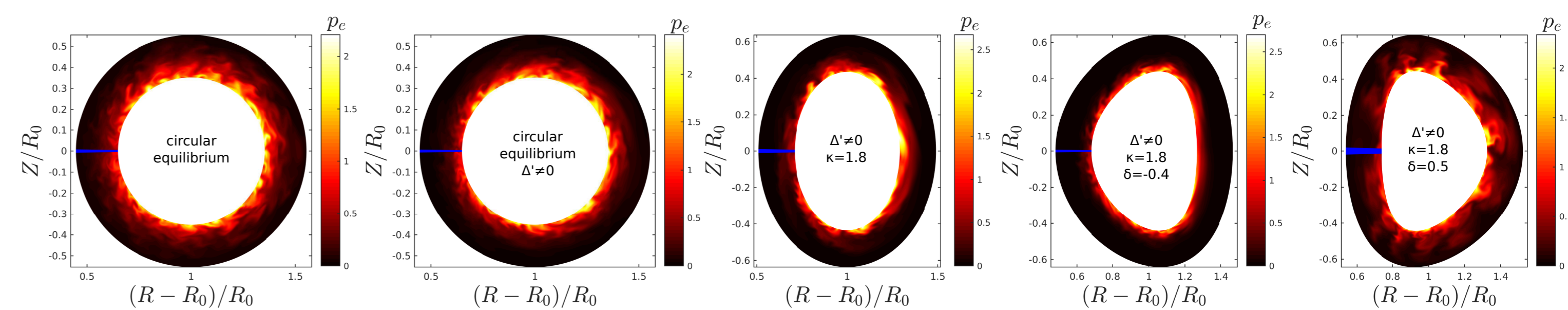


D-shaped equilibrium



## Non-linear simulations

- Fully-turbulent non-linear simulations** with same physical parameters, in **different magnetic geometries**



- Mitigation of turbulence** by  $\Delta'$ ,  $\kappa$ , and **negative**  $\delta$ ; **enhancement of turbulence** by **positive**  $\delta$

## Gradient removal saturation mechanism

- The radial gradient of the **perturbed** plasma pressure **comparable** to the radial gradient of the **background** plasma pressure
- Leading order term of the pressure equation gives the perturbed potential
- Balance** between **radial flux**  $\Gamma_p = \tilde{p} \partial_{\theta} \tilde{\phi}$  and **parallel losses**
- Assuming  $k_r = \sqrt{k_{\theta} / L_p}$  and choosing **linear growth rate**  $\gamma$  and **wavenumber**  $k_{\theta}$  to **maximize the transport**

$$\partial_r \tilde{p} \sim \partial_r \tilde{p} \Rightarrow k_r \tilde{p} \sim \tilde{p} / L_p$$

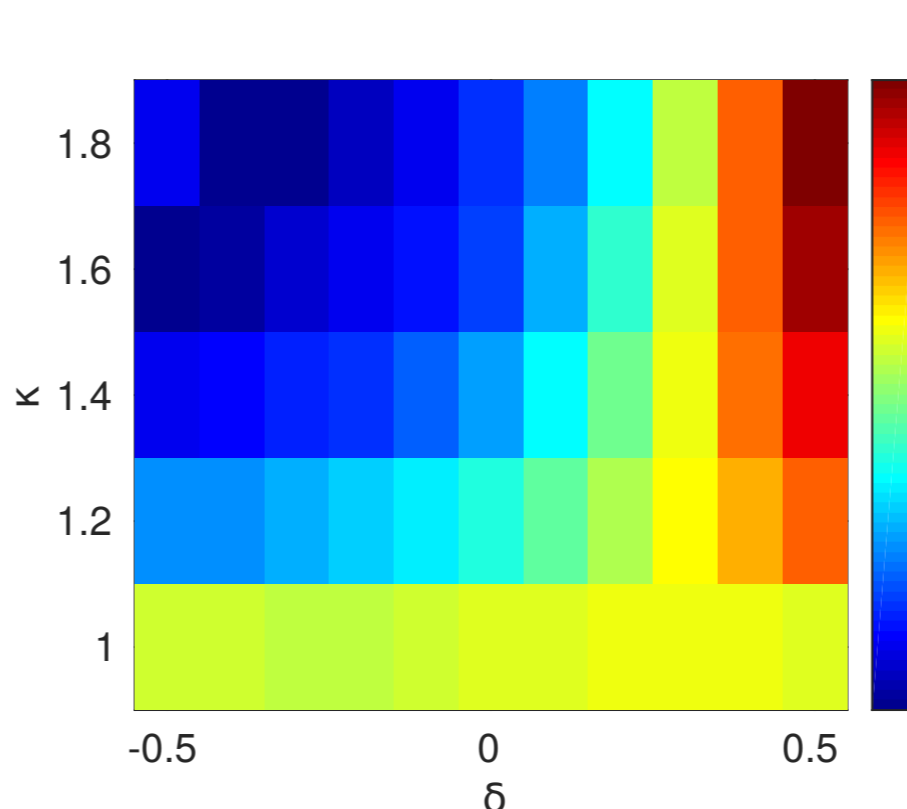
$$\partial_t \tilde{p} \sim \partial_{\theta} \tilde{\phi} \partial_r \tilde{p} \Rightarrow \tilde{\phi} \sim \gamma \tilde{p} L_p / (\tilde{p} k_{\theta})$$

$$\partial_r \Gamma_p \sim \nabla_{\parallel} (\tilde{p} v_{\parallel}) \Rightarrow \Gamma_p / L_p \sim \tilde{p} c_s / (qR)$$

$$L_p \sim \frac{qR}{c_s} \left( \frac{\gamma}{k_{\theta}} \right)_{\max}$$

	circular	circular $\Delta' \neq 0$	$\Delta' \neq 0$ $\kappa = 1.8$ $\delta = -0.4$	$\Delta' \neq 0$ $\kappa = 1.8$ $\delta = -0.3$	$\Delta' \neq 0$ $\kappa = 1.8$	$\Delta' \neq 0$ $\kappa = 1.8$ $\delta = 0.3$	$\Delta' \neq 0$ $\kappa = 1.8$ $\delta = 0.5$
$L_p$ non-linear simulations	31 ± 4	22 ± 4	13 ± 3	14 ± 2	19 ± 2	21 ± 3	27 ± 5
$L_p$ Gradient Removal theory	35	27	18	18	21	27	34

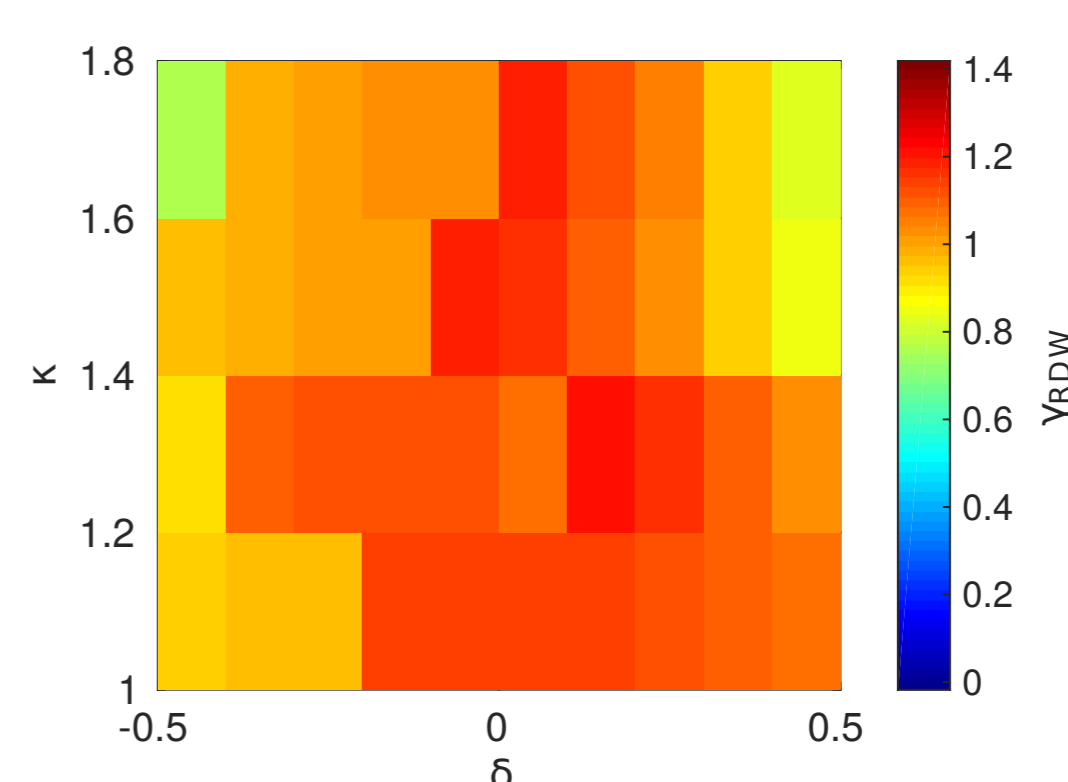
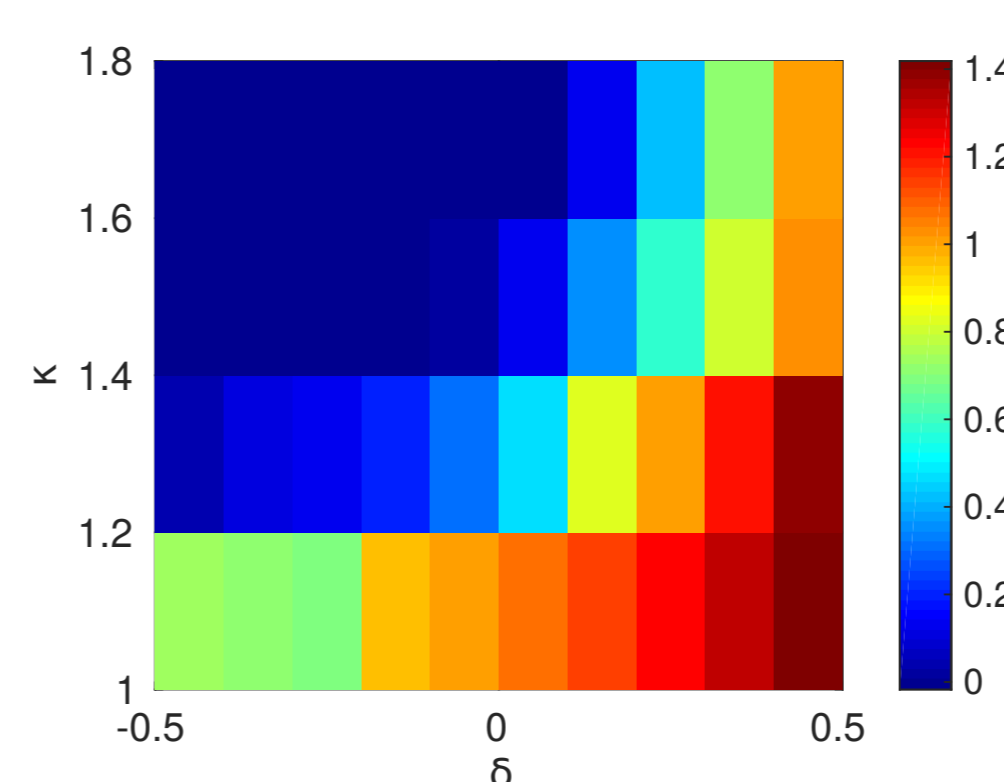
- Good **agreement** between **non-linear simulations** and **Gradient Removal theory**



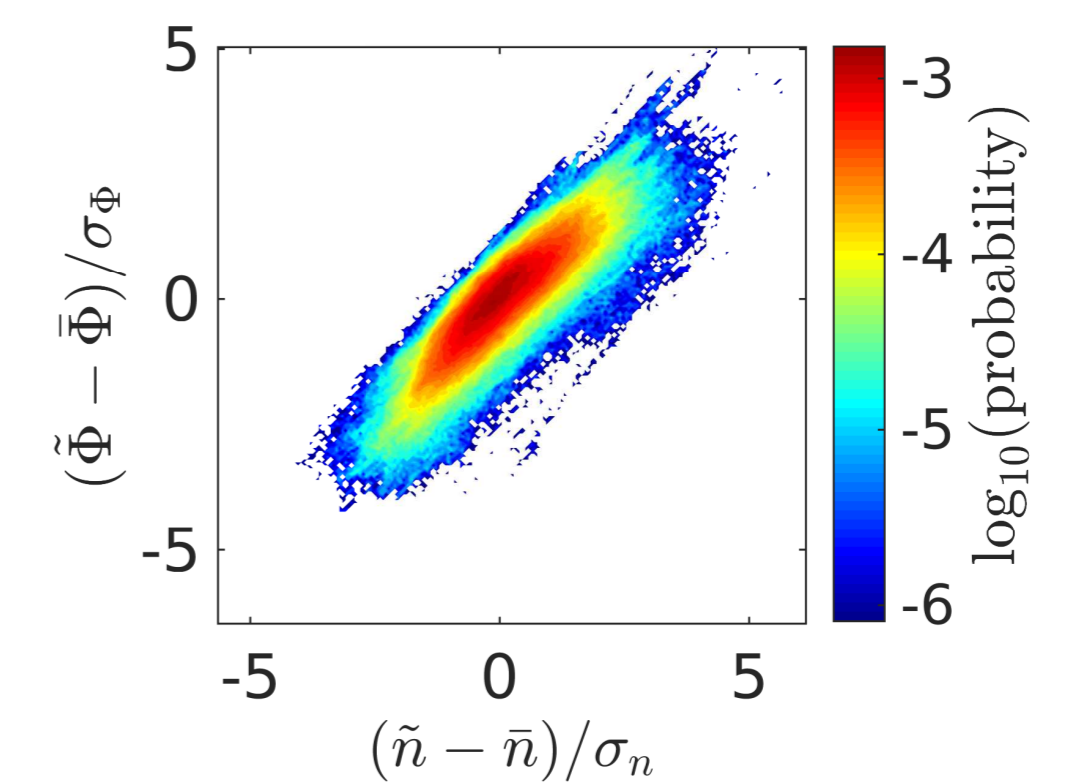
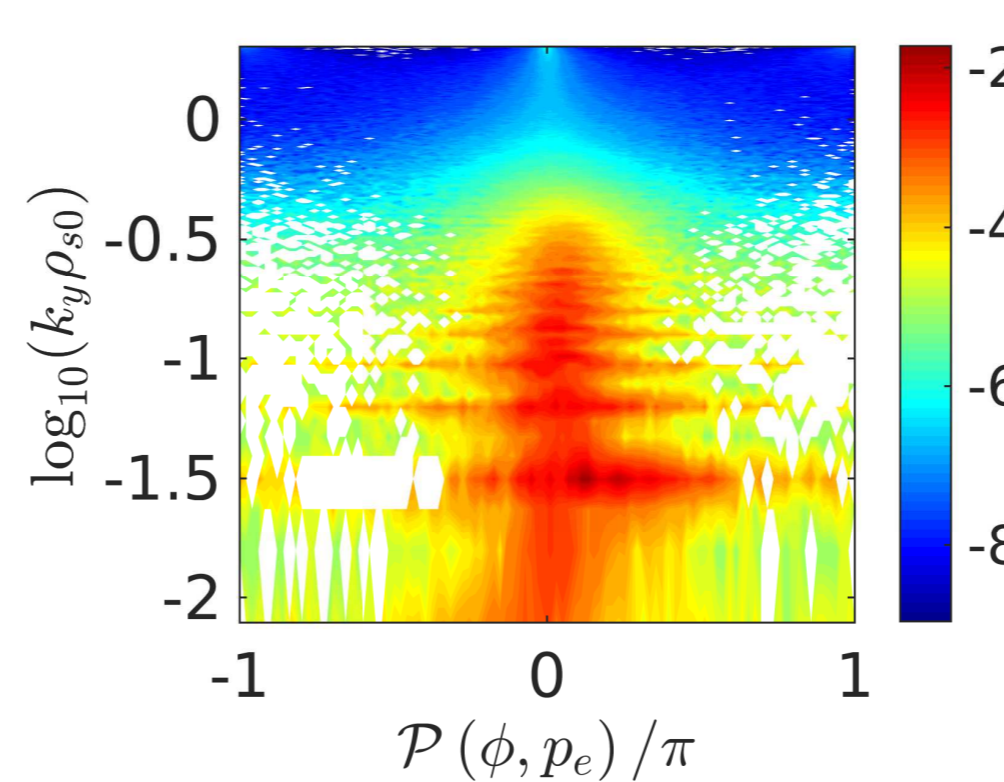
- Linear scan** over  $\kappa$  and  $\delta$  **confirms the trend** observed for the non-linear simulations
- Preliminary study indicates the **curvature** as the **most important operator** in setting  $L_p$

## Non-linear turbulent regimes

- Investigation of the turbulent regimes to **understand the mitigation of turbulence** by  $\kappa$  and negative  $\delta$

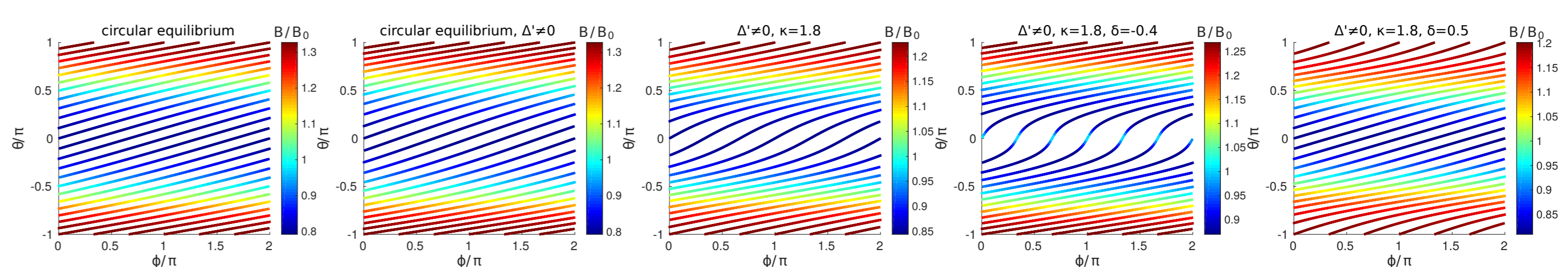


- Resistive ballooning modes mitigated** by  $\kappa$  and negative  $\delta$
- Resistive drift waves slightly affected** by shaping effects



- Non-linear simulations confirm that **turbulence is dominated by drift waves** for negative  $\delta$

- Why** are  $\kappa$  and negative  $\delta$  mitigating ballooning modes?



- Shafranov shift**, **elongation** and **negative triangularity stretch** magnetic field lines near the **outer midplane**
- Positive triangularity compress** magnetic field lines near the **outer midplane**
- Curvature less effective with Shafranov shift, elongation and negative triangularity, and more effective for positive triangularity
- Ballooning modes strongly mitigated** by Shafranov shift, elongation and negative triangularity, **enhanced** by positive triangularity

## Conclusion

- Simulations of SOL turbulence in shaped plasmas
- Scan of  $L_p$  and  $\gamma$  over  $\kappa$  and  $\delta$ , showing how ballooning modes and drift waves are affected by different magnetic configurations
- Qualitative understanding of the mechanism mitigating/enhancing the ballooning character of turbulence